Spectroscopic studies of carbon monoxide: application for detection in flames

O. Carrivain[1], M. Orain[*, 1], N. Dorval[1], C. Morin[2], G. Legros[3,4]

[1]ONERA – The French Aerospace Lab, 91761 Palaiseau, France
[2]LAMIH CNRS UMR 8201, UVHC, Le Mont Houy, 59313, Valenciennes cedex 9, France
[3]Sorbonne Univ, UPMC Univ Paris 06, UMR 7190, Inst Jean Le Rond dAlembert, F-75005 Paris, France
[4]CNRS, UMR 7190, Inst Jean Le Rond d'Alembert, F-75005 Paris, France

Abstract
In this study, we investigated both experimentally and numerically two-photon laser-induced fluorescence from carbon monoxide (CO-TPLIF) in order to determine the applicability of this technique for imaging CO concentration in aircraft combustion chamber. Experiments were carried out in an optical –accessible gas cell under various conditions of temperature (300-900 K), pressure (0.1-3 MPa) and carrier gas (N_2, air, He). Fluorescence intensity decreases as temperature and pressure increase. Comparison between simulations and experimental results show good agreement.

Introduction

Control of pollutant emissions from aircraft engines is crucial for gas turbine manufacturers. Regulations are becoming more and more stringent and, therefore, require drastic reduction of emissions in the coming decade. Among pollutants generated by combustion process, nitrogen oxides (NOx) and carbon oxides (COx) are those which reduction is most needed. Indeed, nitrogen oxides are known to impact human health, while carbon oxides are greenhouse gases. Reduction of these pollutants requires to improve combustion processes (liquid fuel atomisation, air/fuel mixing, etc). Classically, pollutant emissions are measured at the outlet of a combustor using physical probes. However, improving combustion requires to better understand physical phenomena related to pollutant formation and to measure their concentration inside the combustor. Laser diagnostics are perfectly suitable tools for such a purpose because they are non-intrusive, with a good spatial (~ 100 µm) and temporal resolution (~ 10 ns). The most common techniques include Rayleigh scattering [1, 2], Laser-Induced Fluorescence (LIF) [3-5], absorption [6, 7] and spontaneous Raman scattering [1, 8]. LIF is particularly attractive because it allows measurements in gaseous and two-phase flows, which cannot be done easily with Rayleigh scattering. LIF can also be used to image the flow as opposed to line-of-sight absorption measurements. In addition, LIF delivers intense signals compared to those obtained with spontaneous Raman scattering, which leads to better sensitivity. Fluorescence measurements of carbon monoxide molecule (CO) have been the subject of a large number of articles in the literature, either from a purely spectroscopic point-of-view [9, 10], or from combustion applications purposes [11-14]. Nonetheless, these measurements were generally performed at low or atmospheric pressures, which are not necessarily representative of real engine (aircraft or automotive) operation. Additionally, apart from the work of Richter et al. [11] who carried out CO fluorescence imaging, these measurements were only point wise, which is of limited interest in turbulent flows where scalars distributions vary in time and space. In such flows it is indeed desirable to obtain single-shot 2D-maps of scalars (e.g. temperature, concentration, velocity, etc) in order to gather an instantaneous image of the flow properties.

The goal of the present study was firstly to develop a numerical code that simulates excitation and fluorescence spectra of CO molecule. Secondly, detailed spectroscopic measurements were carried out in an optical-accessible gas cell in order to determine the photophysics of CO fluorescence under various conditions of temperature, pressure and carrier gas. This large dataset was also used to validate the numerical code.

Spectroscopic background

The energy levels involved to this study are schematically represented in Fig. 1. Carbon monoxide is two-photon pumped from the ground state ($X^1\Sigma^+$ (v''=0, J'')) to the excited state ($B^1\Sigma^+$ (v'=0, J')). Please note that absorption of a third photon can lead to ionization of CO molecule. The $B^1\Sigma^+$ state can relax by collision or spontaneous emission toward the lower-lying level ($A^1\Pi$(v=0-5, J)) and $X^1\Sigma^+$ state. Additionally, collisions can yield deactivation of the $B^1\Sigma^+$ state to the $b^3\Sigma^+$ triplet state, which can emit fluorescence at a later stage. Fluorescence signal I_{fluo} for B-A transition is given by the following expression, where A<<Q has been assumed:

$$I_{fluo} \propto N_{CO} W_{2\upsilon} \frac{A_{v'v}}{Q + W_i} \qquad (1)$$

where N_{CO} is the total number density of CO [cm^{-3}], $A_{v'v}$ [s^{-1}] the Einstein coefficient for $B^1\Sigma^+$ (v'=0, J')→ $A^1\Pi$(v=0-5, J) transition, Q the quenching rate [s^{-1}], $W_{2\upsilon}$ the two-photon absorption rate in [s^{-1}] and W_i the

* Corresponding author: mikael.orain@onera.fr

ionization rate coefficient [s^{-1}]. The latter two rates are given by:

$$W_{2\upsilon} = \hat{\sigma}^{(2)}\left(I / hc\upsilon_L \right) \quad (2)$$

$$\hat{\sigma}^{(2)} = \sigma_{2\nu} \sum_{J"} F_{J"} S^{(2)}_{J"J"} \times \int_{-\infty}^{+\infty} \Phi_{J"J'}(\xi - \upsilon_{J"J'}) g(\xi - 2\upsilon_L) d\xi \quad (3)$$

$$W_i = \sigma_I \frac{I}{h\upsilon_L} \quad (4)$$

where I ($W.cm^{-2}$) is the intensity of the laser centered at υ_L (Hz) with line shape g, $\upsilon_{J'',J'}$ is the two-photon line position with line shape $\Phi_{J'',J'}$, $\sigma_{2\upsilon}$ (cm^4) is the electronic and vibrational part of the two-photon absorption cross-section and σ_i (cm^2) the ionization cross-section, $S^{(2)}$ is the two-photon Honl-London factor, $F_{J''}$ is the fractional population in the state J''.

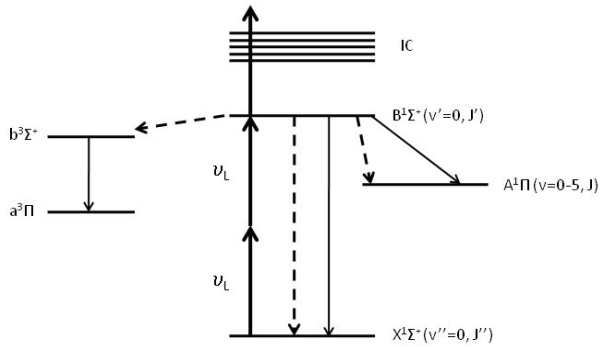

Fig. 1. Energy level relevant and excitation scheme of the fluorescence. Dashed arrow: quenching path; solid arrow: fluorescence emission; IC: ionization continuum.

In order to model CO-TPLIF, a numerical code capable of simulating both excitation and fluorescence spectra has been developed under Matlab® environment.

Two-photon excitation spectra are simulated using Eq (1). The rotational energies of state $X^1\Sigma^+(v''=0)$ and $B^1\Sigma^+(v'=0)$ are calculated using the term energies and the spectroscopic constants from [15, 16]. Based on rotational energies, the lines positions of CO B-X system (Hopfield-Birge Band) are determined using the two-photon selection rules for $^1\Sigma^+$-$^1\Sigma^+$ transition ($\Delta J=0, \pm 2$). These selection rules lead to 3 branches (S, Q and O), for each rotational level J''. For the calculation of line strength, the two-photon absorption cross-section σ_{2v} (electronic and vibrational part in cm^4) is taken from [17], and the two-photon Honl London factors for linear polarization are given by Bray and Hochstrasser [18] for S, Q and O branches, for each J''.

The excitation laser was assumed to have a Gaussian lineshape with full width at half-maximum (FHWM) of 0.7 cm^{-1}. The transition lineshape was calculated using a Voigt algorithm that combines Doppler and collisional broadening. For a two-photon excitation, the Doppler width is equal to $2(\ln(2))^{1/2}(v_p/c)\times 2\upsilon_L$, where v_p is the most probable molecular speed. The collisional width (2γ) and shifting (δ) coefficients and the temperature exponents are taken directly from Ref. [19].

Fluorescence spectra are simulated using Eq (1), for the first six vibrational bands. The rotational energies of $A^1\Pi$ (v=0-5) state are directly taken from Ref. [20]. From rotational energies, the lines positions of CO B-A (Angstrom band) are calculated using one-photon selection rule for $^1\Sigma^+$-$^1\Pi$ transition ($\Delta J=0, \pm 1$). These selection rules lead to 3 branches P, Q and R. For the calculation of emission strengths Einstein coefficient A are taken from Ref. [21], and the Honl London factor from Ref. [22]. Ionization rate (W_i) is computed, using the ionization cross-section measured by Di Rosa and Farrow [23]. The collisional quenching rate is calculated from $Q = \sum_i N_i v_i \sigma(T)$, where N_i is the number density of ith quencher; v_i is the relative velocity and $\sigma(T)$ is the quenching cross-section. The temperature-dependent quenching cross-sections of CO $B^1\Sigma^+(v'=0)$ state in collision with all major species in combustion (N_2, O_2, CH_4, CO, CO_2, H_2O), were measured by Settersten et al [24], at temperatures between 293 K and 1031 K. Based on these measurements, Settersten et al. [24] deduced for each species a power-law for the temperature dependence of quenching cross-section. From the same Voigt algorithm, the fluorescence lineshape has been calculated. The spectrometer resolution was assumed to have a Gaussian lineshape with full width at half-maximum (FHWM) of 1 nm and the collisional width for each rotational line was selected to be $0.1(300/T(K))^{0.5}$.

Experimental set-up

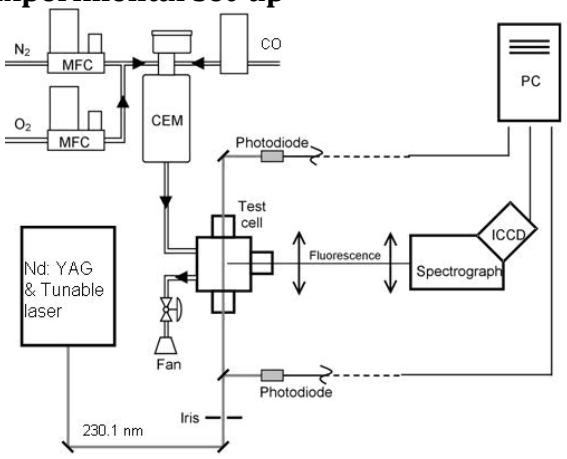

Fig. 2. Experimental set-up for test cell measurements.

An optical-accessible gas cell allowed measurements of CO fluorescence at temperatures between 300 and 900 K, pressures from 0.1 to 1.3 MPa and under different atmosphere (nitrogen, air, helium). The set-up used for experiments is represented in Fig. 2. CO and carrier gas were supplied by pressurized bottles. Gas supply lines were connected to mass flow controllers (MFC) which were used to control mass

flowrates of CO and carrier gas. The outlet of the MFCs were connected to a unique supply line where all gases mixed together, the subsequent mixture was injected into the test cell. The molar fraction of CO in the mixture entering the cell was fixed at 2.6 % in order to keep laser absorption by CO in the test cell to a reasonable level. Temperature of the gas inside the cell was controlled during the fluorescence measurements by means of a type K thermocouple placed a few millimeters aside of the laser probe volume. Temperature values mentioned in thereafter correspond to the gas temperature measured by this thermocouple. Pressure was measured with a pressure transducer (Tb244, JPB) at the output of the test cell. Optical access was provided by three UV-silica windows. Two windows were used for laser access, while fluorescence emitted by CO was recorded through a third window placed at 90° from the propagation of the laser beam.

Spectroscopic experiments were also carried out in a laminar premixed CH_4/air flat flame with equivalence ratio between 1.1 and 1.4, at atmospheric pressure. Fluorescence measurements were performed about 1 mm above the surface of the burner at a location where CO-LIF signal was the largest.

In each experiment, CO molecules were excited by UV pulses from a laser source emitting light at 230.1 nm with a linewidth of 0.7 cm^{-1}. Excitation at 230.1 nm consisted on using the second harmonic of a Nd:YAG laser (YG780, Quantel) at 532 nm to pump a dye laser (TDL50, Quantel) using Rhodamine 610, frequency-doubling the resulting laser beam with a KD*P crystal, then mixing it with the fundamental of the Nd:YAG laser at 1064 nm. Repetition rate of the laser was 10 Hz. The resulting beam was focused into the test cell. In the current experiments, laser energy was kept below 0.4 mJ in order to avoid photolytic decomposition of CO molecules into other compounds.

For recording dispersed fluorescence spectra, fluorescence signal from part of the illuminated CO molecules was collected at right angle by a spectrograph (SPEX 270M, Jobin Yvon) with an entrance slit of 150 µm and a 600 groves/mm grating blazed at 400 nm. The light dispersed by the grating was recorded using a 16-bit intensified CCD camera (Princeton Instrument) with an intensifier gate width of 100 ns. This gate width is about an order of magnitude longer than CO fluorescence lifetime. The CCD array was 576 by 384 pixels and the framing rate of the system was 10 Hz. The ICCD camera was interfaced to a personal computer which was used to control the camera and acquire the spectra. The spectral resolution of the detection system was about 1 nm, which was not enough to distinguish the fine rotational structures in the fluorescence spectrum. However, this resolution allowed detection of shape changes in the fluorescence spectra, for example with the pressure increase.

For each experimental condition, fluorescence and absorption measurements were averaged over 500 laser shots. Absorption cross-section was classically calculated using the absorption's law for two-photon excitation and each fluorescence spectrum was corrected for beam attenuation due to absorption and normalised by laser energy. In addition, all the data shown here are referenced to the same number density. Indeed, despite the flowrates of CO and carrier gas (N_2, air, He) were kept constant for all experimental conditions, the spectra of CO have been corrected for decrease in number density when increasing temperature at fixed pressure, or for increase in number density when increasing pressure at fixed temperature. An equivalent set of measurements was also acquired immediately afterwards with the same laser energy in the cell evacuated from any CO to allow subtraction of background light from fluorescence. Spectra were corrected for the spectral response of the detection system using calibration from the emission spectrum of a deuterium lamp. Temperature (± 1 K tolerance), pressure (± 0.005 MPa tolerance) and CO molar fraction (± 2 % tolerance) were thoroughly controlled and particular attention was paid to perform measurements at steady state conditions.

For recording excitation LIF spectra, laser wavelength around 230 nm was scanned every 0.3 picometer. Laser energy was recorded for each laser shot by a power meter (Nova II, Ophir) in order to correct fluorescence values for the temporal fluctuations of the laser energy. Fluorescence from CO molecules was collected at right angle by a spherical UV lens using a 2f setup to focus fluorescence onto a pinhole placed in front of a photomultiplier tube (XP2018B, Photonis). Spectral filtering of the fluorescence was performed with an interference filter centred at 485 nm with a full width at half maximum of 25 nm and a transmittance larger than 95 %. The filter allowed to record fluorescence from the B(0)-A(1) band around 483 nm. For each laser wavelength of the scanning range, the output signal from the photomultiplier was time-integrated (over 15 ns) by a boxcar (SR250, Stanford Research Systems) and averaged over 30 laser shots. A Labview® interface was used to record both laser energy and integrated fluorescence signals and display the spectra.

Results

The two-photon $B^1\Sigma^+$ (v'=0) ←← $X^1\Sigma^+$ (v''=0) excitation spectrum is characterized by a strong and narrow Q branch having a maximum at 230.104 nm and very weak S and O branches (cf. Fig. 3a). This feature can be explained by the overlap of the *Q* branch lines because of the similar values of the rotational constants for the $B^1\Sigma^+$ (v'=0) state (B_e=1. 9481 cm^{-1}) and the $X^1\Sigma^+$ (v''=0) state (B_e=1. 9225 cm^{-1}). Fluorescence spectrum in Fig. 3b presents a maximum at 519 nm (band B(0)-A(2)). The influence of temperature and pressure on the Q-branch lineshape is investigated later in the paper. In

order to show this influence, each spectrum is normalized to the peak signal. It is noted that temperature and pressure induce a broadening of the Q-branch line shape. Indeed, increasing temperature leads to the apparition of the rotational lines because collisional width decreases with temperature. Additionally, unlike temperature, pressure induces a significant spectral shift on the excitation spectra. Indeed, increasing pressure from 1 to 10 bar shifts the Q-branch by 7 pm towards the longest wavelengths.

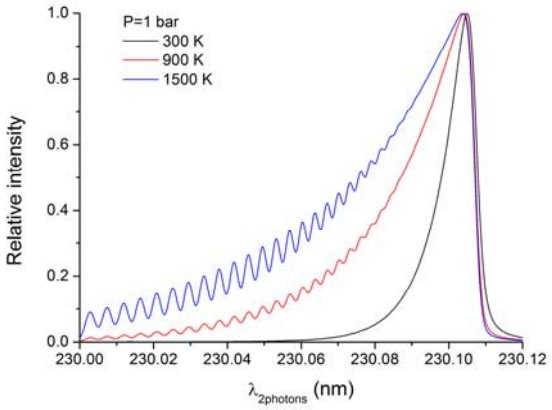

(a)

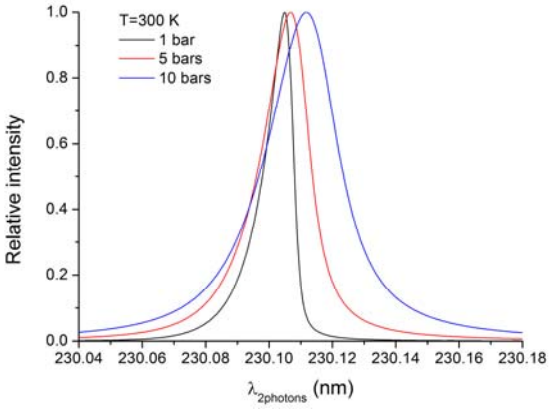

(b)

Fig.3. Influence of temperature (a) and pressure (b) on the Q-branch line shape.

A comparison between simulated and experimental excitation and fluorescence spectra at 300 K and 1 bar is presented in Fig. 4. Both excitation spectrum of Q-branch and fluorescence spectrum were obtained in a mixture composed of 2.6 % CO diluted in N_2/O_2 (with respective molar fractions of 80 % and 20 %). Good agreement between experiment and simulation is observed for both spectra. In particular, the shape and the width of the excitation spectrum are well captured by the simulations. In the fluorescence spectrum, the full width at half maximum of each band is equal to 1.4 nm.

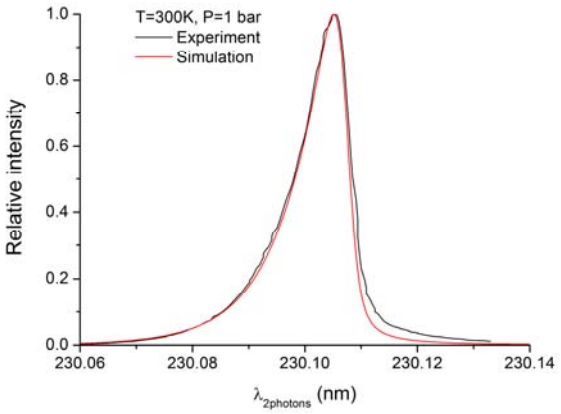

(a)

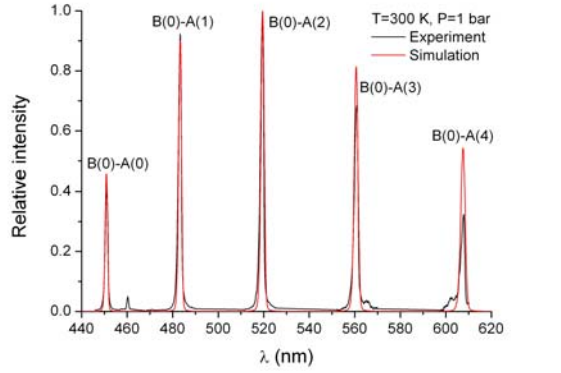

(b)

Fig.4. Comparison between simulation and experiments of excitation (a) and fluorescence (b) spectra at 300 K and 1 bar.

Fig 5 displays the excitation spectrum recorded in a flame with equivalence ratio equal to 1.16. The best fit of the experimental spectrum is obtained from simulations with a temperature of 1750±50 K. This value is similar to that predicted by the PREMIX code [25]. At that temperature, rotational structure is resolved for levels with J>25. Comparison between simulations and experiments is in good agreement. In particular the amplitude of the spectral lines and the distance between each line is well reproduced in the simulations. The CO-LIF code is therefore validated for temperatures in the range 300-1750 K.

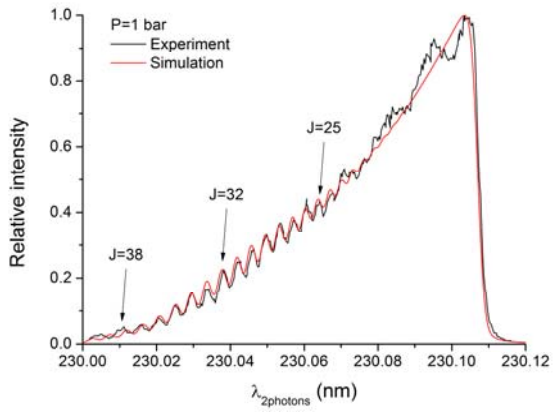

Fig. 5. Comparison between simulation and experiments of integrated fluorescence in flame at 1 bar.

Variation of the integrated fluorescence with temperature at 1 bar and with pressure at 300 K is illustrated in Fig. 6. For each pressure and temperature, integrated fluorescence of the B(0)-A(1) band is normalized by the peak signal. Good agreement is observed for both evolutions with temperature and pressure. The CO-LIF code is therefore validated for pressures in the range 1-13 bars.

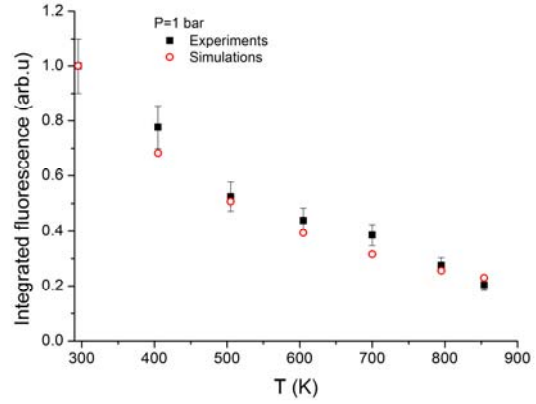

(a)

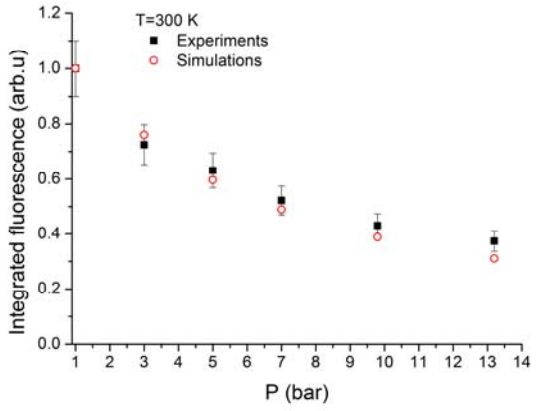

(b)

Fig. 6. Comparison between simulation and experiments of integrated fluorescence as a function of temperature (a) and pressure (b).

Conclusion

In this study, we aimed at better understanding the photophysics of CO molecule. First, a 5-level model was used to simulate excitation and fluorescence spectra of CO molecule. This model takes into account two-photon absorption, ionization process and quenching effects. Second, a large database of CO fluorescence spectra was obtained for different conditions of temperature, pressure and carrier gas from experiments conducted in an optical-accessible gas cell. Fluorescence intensity decreases as temperature and pressure increases. Fluorescence intensity was maximum in Helium which quenching is much lower than N_2 or O_2 molecules. Numerical simulations were validated against experimental results and comparison shows good agreement for the operating conditions investigated in the article. In the future, we will develop CO-PLIF imaging technique in a premixed lab-scale burner operating with methane fuel in order to determine the spatial distribution of CO molecules in a flame.

References

[1] F.Q. Zhao, and H. Hiroyasu, Prog. Energy. Combust. Sci. Technol. **19**, 447 (1993)

[2] F. Fuest, R.S. Barlow, J-Y Chen, A. Dreizler, Combust. Flame. **159**, 2533 (2012)

[3]C. Schulz, V. Sick, J. Wolfrum, V. Drewes, M. Zahn, R. Maly, Twenty-Sixth Symposium (International) on Combustion. 2597 (1996)

[4] M. Orain, P. Baranger, B. Rossow, F. Grish, Appl. Phys. B. **102**, 163 (2011)

[5] M.C. Thurber, F. Grish, B. Kirby, M. Vostmeieir, R.K. Hanson, Appl. Opt. **37**, 4963 (1998)

[6] B. Rosier, P. Gicquel, D. Henry, A. Coppalle, Appl. Opt. **27**, 360 (1988)

[7] A. Mohamed, B. Rosier, D. Henry, Y. Louvet, PL Varghese, AIAA Journal **34, 494** (1996)

[8] J. Kojima, and Q –V Nguyen, Meas. Sci. Technol. **19,** 015406 (2008)

[9] R. A. Bernheim, C. Kitrell, D.K. Veirs, Chem. Phys. Letters. **51**, 325 (1977)

[10] S. V. Filseth, R. Wallenstein, R.H. Zacharias, Opt. Commun. **23**, 231-235 (1977)

[11] M. Richter, ZS. Li, M. Aldén, Appl. Spectrosc. **61**, 1 (2007)

[12] J. M. Seitzman, J. Haumann, R.K. Hanson, Appl. Opt. **26**, 2892 (1987)

[13] M. Mosburger, and V. Sick, Appl. Phys. B. **99**, 1 (2010)

[14] B.J. Kirby, and R. K. Hanson, Appl. Phys. B. **69**, 505 (1999)

[15] T. D. Varberg, and K. M. Evenson, Astrophys. J. **385**, 763 (1992)

[16] C. Amiot, J-Y Roncin, J. Verges, J. Phys. B. : At. Mol. Phys. **19**, L19 (1986)

[17] M. D. Di Rosa, and R.L. Farrow, J. Opt. Soc. Am. B. **16**, 1988 (1999)

[18] R.G. Bray, and R. M. Hochstrasser, Mol. Phys. **31**, 1199 (1976)

[19] M. D. Di Rosa, and R.L. Farrow, J. Spectrosc. Radiat. Transfer. **68**, 363 (2001)

[20] A. Le Floch, J. Mol. Spectrosc. **155**, 177 (1992)

[21] M. Lino da Silva, and M. Dudeck, J. Spectrosc. Radiat. Transfer. **102**, 348 (2006)

[22] G. Herzberg, "Molecular Spectra and molecular structure, I. Spectra of diatomics molecules" New York : Princeton, 1965

[23] M. D. Di Rosa, and R. L. Farrow, J. Opt. Soc. Am. B. **16**, 861 (1999)

[24] T.B Settersten, A. Dreizler, R.L. Farrow, J. Chem. Phys. **117**, 3173 (2002)

[25] R.J. Kee, F.J. Grear, M.D. Smooke, J.A. Miller, Sandia Report No. SAND85-8240, Sandia National Laboratories (1985)